Journal of Alloys and Compounds 762 (2018) 282–288

Contents lists available at ScienceDirect

Journal of Alloys and Compounds

journal homepage: http://www.elsevier.com/locate/jalcom

A fine-grained and low-loss X8R $(Ba_{1-x}Dy_x)(Ti_{1-x/2}Ca_{x/2})O_3$ ceramic

Da-Yong Lu [a, *], Shan Yin [a, b], Shu-Zhen Cui [a, c]

[a] Key Laboratory for Special Functional Materials in Jilin Provincial Universities, Jilin Institute of Chemical Technology, Jilin, 132022, PR China
[b] School of Pharmacy, Shanghai Jiao Tong University, Shanghai, 200240, PR China
[c] College of Chemistry, Northeast Normal University, Changchun, 130024, PR China

ARTICLE INFO

Article history:
Received 27 February 2018
Received in revised form
21 April 2018
Accepted 15 May 2018
Available online 18 May 2018

Keywords:
A. Ceramics
B. Solid state reactions
C. Dielectric response
D. X-ray diffraction
D. Electron paramagnetic resonance

ABSTRACT

$(Ba_{1-x}Dy_x)(Ti_{1-x/2}Ca_{x/2})O_3$ (BDTC) ceramics were prepared at 1400 °C using the solid-state reaction method. The solubility limit was determined by XRD to be $x = 0.15$. The BDTC ceramic with $x = 0.10$ exhibited a high relative density (95%), a fine-grained microstructure (1.2 μm), X8R dielectric stability ($|(\varepsilon' - \varepsilon'_{RT})/\varepsilon'_{RT}| \leq 15\%$ in a range −55 to 150 °C), and a lower loss ($\tan\delta < 0.02$) below 2×10^4 Hz. Ferroelectric and paraelectric phases coexist in a wide temperature region. The mixed A and B occupancy for Dy^{3+} and Ca^{2+} ions was proposed to be responsible for the X8R stability associated with double diffused dielectric peaks.

1. Introduction

In the dielectric field, $BaTiO_3$-based ceramics prevail in multilayer ceramic capacitor (MLCC) and become a pillar of electronic ceramic industry [1]. Core-shell structured ceramics satisfying the Electronic Industry Association (EIA) X7R dielectric specification ($|(\varepsilon' - \varepsilon'_{RT})/\varepsilon'_{RT}| \leq 15\%$ in a temperature range from −55 to 125 °C) is widely applied in the MLCC industry for miniaturization of electronic components attributed to their temperature-stable dielectric behavior and the use of base metal electrode (BME) in cost reduction [1–3]. However, there is ever-growing need to extend the upper working temperature of X7R ceramics to 150 °C [4–11] (i.e. X8R specification: $|(\varepsilon' - \varepsilon'_{RT})/\varepsilon'_{RT}| \leq 15\%$ in a range from −55 to 150 °C) or higher temperatures (200–400 °C) [12–15] for the applications of engine electronic control unit (ECU), anti-lock brake system (ABS), and programmed fuel injection (PGMFI) in the automotive field. In recent years, some X8R [4–11] and ultra-broad working temperature ceramics [12–15] were successively developed, such as $BaTiO_3$–$MgCO_3$–MnO_2–rare earth elements (La, Pr, Gd, Tb, Ho, Er, Yb, Lu) [4], $BaTiO_3$–Yb_2O_3–MnO_2 [5], Nb–Co co-doped $BaTiO_3$–$(Bi_{0.5}Na_{0.5})TiO_3$ [6], Nd-doped $xBiAlO_3$–$(1-x)BaTiO_3$ [7], La-doped $BaTiO_3$ [8,9], $BaTiO_3$@La_2O_3@SiO_2 [10], $(Ba_{0.985}Bi_{0.01})TiO_3$–$Ba(Ti_{0.9}Zr_{0.1})O_3$ [11], and $(BaTiO_3$–$(Bi_{0.5}Na_{0.5})TiO_3$-based ceramics [12–15]. Core-shell structured ceramics are usually fabricated under lower sintering temperatures ($T_s \leq 1300$ °C). However, the lower sintering temperature is detrimental to densification of ceramics. For this reason, the sintering aids such as $BaSiO_3$ [5], glass powders and CeO_2 [14,15], are often used to reduce porosity and promote density of ceramics.

In 2014, an simple X8R $(Ba_{1-x}La_x)(Ti_{1-x/2}Ca_{x/2})O_3$ ($x = 0.06$) (BLTC) ceramic sintered at $T_s = 1400$ °C was reported [16]. The larger Ca^{2+} ions in BLTC can be successfully incorporated onto the B-sites *via* the exclusive occupations of La^{3+} at the A-sites [17,18]. However, the X8R application of this ceramic is limited by its higher porosity and dielectric loss ($\tan\delta = 0.06$) [16].

To overcome the above shortcomings in BLTC, we designed and developed three novel X8R $(Ba_{1-x}Dy_x)(Ti_{1-x/2}Ca_{x/2})O_3$ (BDTC) ceramics without the use of sintering aids in 2014 and applied for a country patent of invention for three samples with $x = 0.10$, 0.12, and 0.15. Little information about BDTC was opened in this patent. The origin of X8R stability in BDTC is an academically valuable critical scientific issue. Subsequently, we abandoned the further application of this patent and made wide investigations. By comparison with BLTC, BDTC with $x = 0.10$ exhibited many advantages of higher relative density, homogenous and fine-grained microstructure, and lower dielectric loss. In this work, the characteristics of BDTC solid solution formation were reported. The sintering temperature of $T_s = 1400$ °C can destroy core-shell structure and

* Corresponding author. Tel.: +86 432 62185308; fax: +86 432 63093625.
E-mail addresses: cninjp11232000@yahoo.com, dylu@jlict.edu.cn (D.-Y. Lu).

https://doi.org/10.1016/j.jallcom.2018.05.171
0925-8388/

result in the complete incorporations of Dy/Ca ions in the $BaTiO_3$ lattice. The origin of X8R stability and additional features were clarified.

2. Experimental

2.1. Synthesis

The ceramic raw materials were reagent-grade $BaCO_3$ (99.4%), $CaCO_3$ (99.5%), TiO_2 (99.5%), and Dy_2O_3 (99.9%) powders. Ceramics were prepared according to the nominal formula of $(Ba_{1-x}Dy_x)(Ti_{1-x/2}Ca_{x/2})O_3$ ($x = 0.04$, 0.06, 0.08, 0.10, 0.15, 0.16, 0.18, 0.20) (BDTC) using a previously published solid-state reaction method [16]. The final sintering conditions were chosen to be 1400 °C for 12 h with a heating rate of 100 °C/h and a cooling rate of −200 °C/h to 1000 °C followed by furnace cooling to room temperature (RT). BDTC ceramics with $x = 0.04$ (BD4TC) were prepared at 1250, 1300, 1350, and 1400 °C for 12 h for monitoring of solid solution formation. In addition, because the solubility limit of Dy in $Ba(Ti_{1-x}Dy_x)O_{3-x/2}$ ceramics sintered at 1400 °C for 72 h was indicated by Makovec et al. to be $x = 0.15$ [20], $Ba(Ti_{0.96}Dy_{0.04})O_{2.98}$ (BTD4) ceramic with O vacancies was prepared according to Makovec et al.'s experimental route for EPR detection of oxygen vacancies and comparison.

2.2. Characterization

Powder X-ray diffraction (XRD) data were recorded at RT using a DX-2700 X-ray diffractometer (Dandong Haoyuan). Lattice parameters were calculated with MS Modeling (Accelrys Inc.) using Rietveld refinement and Cu $K\alpha_1$ radiation ($\lambda = 1.540562$ Å). The Raman spectra were recorded at RT using a LabRAM XploRA Raman spectrometer (Horiba Jobin Yvon) at a laser excitation of 532 nm. The accumulation time and resolution are 2 s and 2.7 cm^{-1}, respectively. Electron paramagnetic resonance (EPR) measurements were performed at RT using an A300-10/12 X-band spectrometer (Bruker) operating at 9.84 GHz. The EPR cavity of the spectrometer was changed with an ER 4102ST cavity for temperature-dependent EPR measurement, X-band frequency: 9.43 GHz. The gyromagnetic factor (g) was calculated by the relationship $h\nu_0 = g\beta H$, where h is the Planck constant ($h = 6.626 \times 10^{-34}$ J s), ν_0 is the microwave frequency, β is the Bohr magnetron ($\beta = 9.262 \times 10^{-24}$ J/T), H is the magnetic field strength. The surfaces of ceramics were polished and then thermally etched to observe the microstructure using an EVOMA 10 scanning electron microscope (SEM) (Zeiss) operated at 15 keV. An Aztec 2.3 energy dispersive spectrometer (EDS) (Oxford Ins.) was attached to the SEM for compositional analyses. The average grain size (GS) was obtained from measurements of the number of grains per unit area on a polished surface (N_A) using Fullman's method, i.e. $GS = (6/\pi N_A)^{1/2}$ [19]. The dielectric properties of ceramics were investigated at 1 kHz using a Concept 41 Dielectric/Impedance spectrometer (Novocontrol) with an applied voltage of 1 V. The accuracy in the measurements of dielectric permittivity, dielectric loss, and temperature control are less than 5%, 3×10^{-5}, and ±0.3 °C, respectively.

3. Results

3.1. Monitoring of solid solution formation

Composition $(Ba_{1-x}Dy_x)(Ti_{1-x/2}Ca_{x/2})O_3$ ($x = 0.04$) (BD4TC) was selected for monitoring of complete solid solution formation. BD4TC shrank continuously with increasing T_s and the relative density (i.e. the ratio of the density (mass of a unit volume) to the theoretical density of a ceramic) increased linearly from 75% at $T_s = 1250$ °C to 92% at $T_s = 1400$ °C. The XRD patterns of BD4TC sintered at $T_s = 1250$–1400 °C are shown in Fig. 1. BD4TC consisted of the main perovskite phase and a small amount of the secondary phases of $Dy_2Ti_2O_7$ and Dy_2O_3 below $T_s = 1350$ °C. A monophasic solid solution without any secondary phase could be formed at $T_s = 1400$ °C and it had a tetragonal perovskite structure, as marked clearly by the characteristic (002)/(200) peak splitting (Fig. 1 insets). Thus, a higher relative density and a tetragonal structure with clear (002)/(200) XRD peak splitting are characteristic of solid solution formation in BD4TC.

3.2. Evolution in crystalline structure of BDTC

The XRD patterns of $(Ba_{1-x}Dy_x)(Ti_{1-x/2}Ca_{x/2})O_3$ (BDTC) ceramics sintered at $T_s = 1400$ °C are shown in Fig. 2a. BDTC exhibited a monophasic perovskite structure up to $x = 0.15$. They were tetragonal for $x \le 0.06$ and pseudo-cubic for $0.08 \le x \le 0.15$. A small amount of a secondary phase, which was assigned to Dy_2O_3, could be observed for $x \ge 0.16$. Thus, the solubility limit in BDTC was determined by XRD to be $x = 0.15$.

The variations in parameters (a, c) and unit cell volume (V_0) as a function of x for BDTC are shown in Fig. 2b and c. The V_0 of BDTC is greater than that of tetragonal $BaTiO_3$ ($V_{0BT} = 64.41$ Å^3, from JCPDS Cards No. 6–526) but far less than that of the cubic $BaTiO_3$ ($V_0 = 65.50$ Å^3, from JCPDS Cards No. 31–174). The V_0 increased with increasing x for $x \ge 0.06$. The V_0–x relation does not strictly satisfy Vegard's law (Fig. 2c).

3.3. Dielectric properties of BDTC and X8R dielectric-temperature stability of BD10TC

The temperature dependences of the dielectric permittivity (ε') and the dielectric loss ($\tan\delta$) for BDTC are shown in Fig. 3. Accompanied by an evolution in crystalline structure with x, the

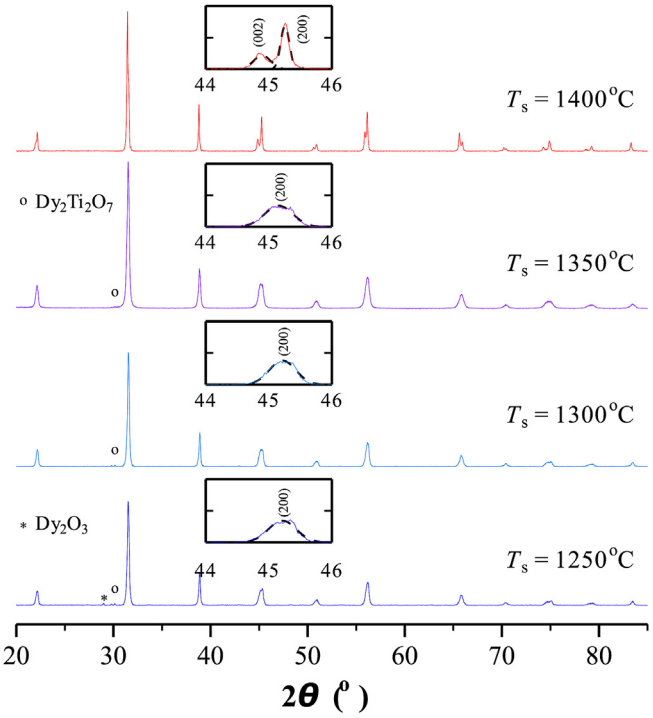

Fig. 1. XRD patterns of $(Ba_{1-x}Dy_x)(Ti_{1-x/2}Ca_{x/2})O_3$ ($x = 0.04$) (BD4TC) ceramics sintered at $T_s = 1250$–1400 °C. The insets depict the enlarged peaks in the vicinity of 45°.